Broadband terahertz polarization beam splitter based on subwavelength grating sandwiched between silica layers

Zhang Yelan[1], Zhang Kun[1], Kong Weijin[1,2], Li Caiyu[1], Xia Feng[1], Yun Maojin[1]

(1. College of Physics Science, Qingdao University, Qingdao 266000, China;
2. Shandong Society for Optical Engineering, Qingdao 266000, China)

Abstract: A broadband terahertz (THz) polarization beam splitter (PBS) was proposed. The PBS was based on subwavelength grating sandwiched between silica layers, which could split an arbitrarily polarized optical beam into two orthogonal, linearly polarized components, and then reflected the TE mode and transmit the TM mode. It was shown that THz PBS could efficiently operate from 3.5 THz to 5.5 THz, with high diffraction efficiencies and extinction ratios. In the process of PBS manufacture, there would be unavoidable deviations of the geometric parameters, which may affect its properties, i.e. the diffraction efficiencies and extinction ratios. Therefore, some structure parameters were calculated. Those values suggested that the designed PBS allows sufficient manufacture tolerances. When D_1 ranged from 1 μm to 1.2 μm and thickness D_3 ranged from 2.8 μm to 3 μm, the values of T_0^{TM} are always more than 96.9% and those of R_0^{TE} are more than 98.7%. And the values of T_c and R_c were respectively kept higher than 31 dB and 33.4 dB. These results show the PBS with a frequency bandwidth of 2 THz, a large angle range of 10°, an extinction ratios over 20 dB and a diffraction efficiencies over 90%, is obtained. This work may inspire related studies and achieve some potential applications in THz manipulation system.

Key words: polarization beam splitter; terahertz device; subwavelength grating

CLC number: O439 **Document code:** A **DOI:** 10.3788/IRLA201948.0520003

基于二氧化硅薄膜夹层式亚波长金属光栅的宽波段太赫兹偏振分束器

张晔岚[1],张 昆[1],孔伟金[1,2],李采彧[1],夏 峰[1],云茂金[1]

(1. 青岛大学 物理科学学院,山东 青岛 266000; 2. 山东省光学工程学会,山东 青岛 266000)

摘 要: 设计出一种结构新颖的宽波段太赫兹偏振分束器,这种偏振分束器由夹层式亚波长金属光栅制成。亚波长金属光栅偏振分束器可以将入射的任意自然光分成两束偏振状态垂直的线偏振光。其中,TE 模反射而 TM 模透射。设计的偏振分束器在 3.5~5.5 THz 波段可以达到很高的衍射效率与消光比。但是,在光栅的实际制作过程中,加工技术的缺陷引起的误差大大影响了光栅的性能,比如衍射效率,消光比等。因此文中对一些结构参数进行了计算,从计算结果可以看出这种偏振分束器也有很好的

收稿日期: 2018-12-07; **修订日期:** 2019-01-13

基金项目: 国家自然科学基金(11274188)

作者简介: 张晔岚(1992-),女,硕士生,主要从事太赫兹波段金属光栅方面的研究。Email:726487797@qq.com

导师简介: 孔伟金(1976-),男,教授,博士生导师,博士,主要从事介质膜金属光栅方面的研究。Email:kwjsd@163.com

工艺容差。当覆盖层厚度 D_1 与底层介质厚度 D_3 的变化范围分别为 1~1.2 μm 和 2.8~3 μm 时，T_0^{TM} 大于 96.9%，R_0^{TE} 大于 98.7%。T_c 和 R_c 分别大于 31 dB 和 33.4 dB。结果显示，设计的偏振分束器在 2 THz 的带宽 10°的大角度范围内，衍射效率高于 90%，消光比大于 20 dB。因此文中设计对于太赫兹调制器件的研究，以及太赫兹通信系统的集成都有很大的参考价值。

关键词：偏振分束器； 太赫兹器件； 亚波长光栅

0 Introduction

Terahertz (THz) electromagnetic waves whose frequencies range from 0.1 to 10 THz have attracted extensive interests due to their broad applications, such as advanced imaging, medical sciences, and national security. As a result, there are rapidly growing demands for THz devices to generate THz waves and manipulate their propagation. Recently, some considerable progresses have been made to develop THz devices, such as THz sources[1-3], phase modulators[4-5], lenses[6-7], beam splitters[8-15] and detectors[16-17]. Polarization beam splitter(PBS) is one of the most important devices to modulate the polarized THz wave. Conventionally, PBS can be designed using birefringent crystals[8-9]. However, natural crystals operating in THz frequencies are very rare and expensive, and not conducive to actual production and all-optical integration. In view of these disadvantages and the urgent needs of terahertz technology development, some researchers have tried to artificially design THz PBS using microstructures and made some achievements. Utilizing elaborately designed liquid crystals[10], two-dimensional photonic crystals[11-12], multilayers structure[13], and subwavelength gratings [14-15], different THz PBSs have been realized and most of them can function with a broad band around 1 THz. Here, based on the inspiration of these work, we design a new THz PBS operating in a broader band by combining the subwavelength grating with the multilayer structure.

In this paper, a new PBS device is designed based on subwavelength grating sandwiched between silica layers[18-19] operating in THz region. Numerical results are achieved by rigorous coupled wave analysis (RCWA)[20] and genetic algorithm (GA)[21] methods, showing that the PBS is a broadband device efficiently operating from 3.5 THz to 5.5 THz. In the working band, the PBS reaches high diffraction efficiency (>90%) and possesses large extinction ratio (>20 dB). In addition, by sweeping the geometric parameters, we find that the designed PBS allows sufficient manufacture tolerance. Such a PBS device with high diffraction efficiency in a broad band may achieve some applications in THz wave manipulation.

1 Design theory

The designed PBS is shown in Fig.1, where the grating is made of steel (ε=837.9−879.68i), filled with SiO_2 (n=1.46) in the groove, and sandwiched by two SiO_2 films on glass (n=1.52) substrate. The labels D_1, D_2 and D_3 respectively represent the thickness of

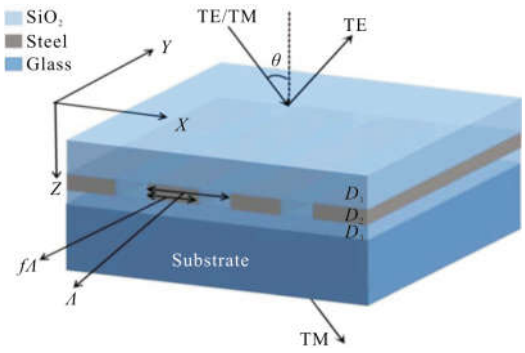

Fig.1 Schematic description of the PBS based on steel subwavelength grating sandwiched between silica layers. D_1 is the top silica layer thickness, D_2 is the groove depth, D_3 is the bottom silica thickness, is the period of grating, and $f\Lambda$ is the length of grating

the top SiO_2 layer, the grating and bottom SiO_2 layer; f, θ and Λ respectively represent the duty cycle, incident angle and the grating period, where f is defined to be the length of grating divided by the grating period Λ. The simple multilayer and grating structure can easily separate incident waves and enhance transmission [22]. If the incident wave is polarized along the grating direction, the conduction electrons are driven along the length of the grating with unrestricted movement. The coherently excited electrons generate a forward-traveling as well as a backward-traveling wave, with the forward-traveling wave canceling the incident wave in the forward direction. The physical response of the grating is essentially the same as that of a thin metal sheet. As a result, the incident wave is totally reflected and nothing is transmitted in the forward direction. In contrast, if the incident wave is polarized perpendicular to the grating and if the grating spacing is smaller than the wavelength, the Ewald-Oseen field generated by the electrons is not sufficiently strong to cancel the incoming field in the forward direction. Thus there is considerable transmission of the incident wave. The backward-traveling wave is also much weaker, leading to a small reflectance. Thus most of the incident light is transmitted.

The diffraction efficiency is one of the most important parameters to evaluate the PBS, which is defined as:

$$\eta_m=\frac{|s_{zm}|}{|s_{z,\mathrm{Inc}}|} \tag{1}$$

where s_{zm} and $s_{z,\mathrm{Inc}}$ are the energy flux along z-axis of the diffraction wave and incident wave, respectively. In this paper, we use T_0^{TE} and T_0^{TM} to represent the transmission efficiency of TE mode and TM mode, R_0^{TE} and R_0^{TM} to represent the reflection efficiency of TE mode and TM mode, respectively. In this way, higher R_0^{TE} and T_0^{TM} correspond with lower loss and better PBS. In addition, the extinction ratio is another important parameter of the PBS, where the transmission extinction ratio T_c and reflection extinction ratio R_c are defined as follows:

$$T_c=10\log_{10}\left(\frac{T_0^{\mathrm{TM}}}{T_0^{\mathrm{TE}}}\right) \tag{2}$$

$$R_c=10\log_{10}\left(\frac{R_0^{\mathrm{TE}}}{R_0^{\mathrm{TM}}}\right) \tag{3}$$

where higher T_c and R_c imply better performance.

Using the rigorous coupled wave analysis (RCWA) method, we can calculate the η_m, T_c and R_c. Here, we divide the system into three regions, the incident region in air, the sandwiched grating region, and the transmission region in substrate. In the sandwiched grating region, to simplify the calculation process, the dielectric film can be regarded as a grating whose period equals to the embedded grating but the duty cycle equals to 1.

In order to optimize the diffraction efficiency of the PBS, we introduce the following optimization function:

$$F=\{\frac{1}{N}\sum_{H_i}[\left(\frac{1}{T_0^{\mathrm{TM}}(H_i)}\right)^2+\left(\frac{1}{R_0^{\mathrm{TE}}(H_i)}\right)^2+(T_0^{\mathrm{TE}}(H_i))^2+(R_0^{\mathrm{TM}}(H_i))^2]\}^{1/2} \tag{4}$$

where H_i represents the frequency, and N is the number of frequencies in calculation. Here, we set the frequencies spanning from 3.5 THz to 5.5 THz with an interval of 0.02. Therefore, N equals to 100 in Eq.(4). In this way, the smaller the F value, the better the performance of the PBS is.

In order to optimize the PBS, we sweep the parameters $\{D_1, D_2, D_3, f, \Lambda\}$ from {2, 1, 0.5, 0.25, 5} to {5, 4, 1.5, 0.45, 7} utilizing the RCWA and the GA. Reasonable optimization range is extremely important. The GA will randomly select a set of initial values, and according to the objective function F in Eq.(4), it picks out the optimal individual using the genetic operators, i.e. select, crossover and mutation. As a result, we finally get the optimized combination of the geometric parameters to be {2.9, 1.91, 1.12, 0.34, 6}, as shown in Tab.1.

Tab.1 Optimized parameter of the PBS for H=4.5 THz, θ=70°

D_1/μm	D_2/μm	D_3/μm	f	Λ/μm
2.9	1.91	1.12	0.34	6

2 Results and discussions

2.1 Simulation results

Based on the optimized geometric parameters, we calculate the diffraction efficiencies and the extinction ratios to examine the performance of the PBS. When the incident angle is 70°, the diffraction efficiencies as a function of frequencies are shown in Fig.2 (a). Using the compression coordinate, we could clearly observe the change of data. The values of R_0^{TE} are higher than 98.4% from 3.5 THz to 5.5 THz, and the values of T_0^{TM} are from 97% to 95.6% in the same frequency range. Moreover, around the center frequency, the values of T_0^{TM} and R_0^{TE} are both higher than 96%. Figure 2(b) exhibits the relationship between the diffraction efficiencies and frequencies. The values of T_c are more than 28.5 dB in the frequency range from 3.5 THz to 5.5 THz. Furthermore, R_c keeps more than 23.1 dB in this range, and even reaches 59.9 dB around the central frequency.

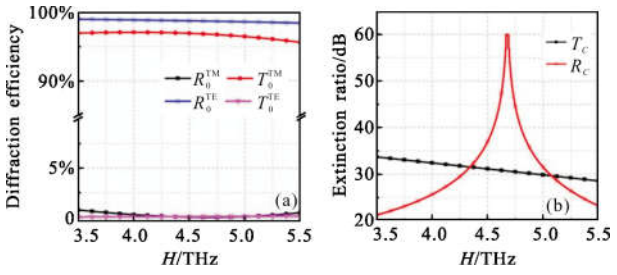

Fig.2 (a) The diffraction efficiencies and (b) the extinction ratios versus the incident frequencies of the PBS with f=0.34, Λ=6 μm, D_1=2.9 μm, D_2=1.91 μm, and D_3=1.12 μm, operating at θ=70°

Figure 3 (a) shows the variation of diffraction efficiency with incident angle around 4.5 THz. The values of T_0^{TM} and R_0^{TE} respectively maintain more than 94% and 98.2% when the incident angles range from 60° to 70°. As shown in Fig.3 (b), when incident angle ranges from 60° to 70°, the values of T_c are more than 29.2 dB. Meanwhile, within the angle range from 64.8° to 73.5°, R_c retains more than 20 dB, and reaches 38.3 dB at the incident angle of 69.7°.

In addition, we calculate the simulation results in Tab.2 and Tab.3, when the values of D_1 and D_1 are 0, the subwavelength grating sandwiched between silica layers can be regard as an ordinary subwavelength grating. Comparing Fig.2, Fig.3 with Tab.2 and Tab.3, it can be clearly seen that the transmittance and extinction ratios of the sandwich grating are much better than ordinary grating.

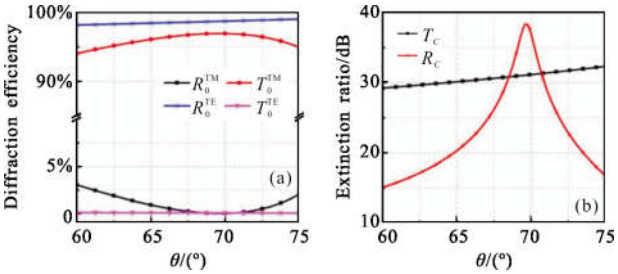

Fig.3 (a) The diffraction efficiencies (b) the extinction ratios versus the incident angles of the PBS with f=0.34, Λ=6 μm, D_1=2.9 μm, D_2=1.91 μm, and D_3=1.12 μm, operating at H=4.5 THz

Tab.2 Results of the PBS with D_1=0, D_3=0, f=0.34, Λ=6 μm, D_2=1.91 μm, operating at θ=70°

H	3.5/THz	4/THz	4.5/THz	5/THz	5.5/THz
T_0^{TM}	82.51%	80.33%	78.44%	76.94%	75.96%
R_0^{TE}	90.96%	90.32%	91.05%	92.44%	93.78%
T_c/dB	17.64	16.75	16.56	16.81	17.24
R_c/dB	8.48	7.86	7.45	7.20	7.11

Tab.3 Results of the PBS with D_1=0, D_3=0, f=0.34, Λ=6 μm, D_2=1.91 μm, operating at H=4.5 THz

θ	60°	65°	70°	75°
T_0^{TM}	89.97%	85.63%	84.28%	82.51%
R_0^{TE}	98.63%	98.85%	98.85%	98.97%
T_c/dB	30.12	30.68	30.82	30.98
R_c/dB	11.16	9.15	8.68	8.13

These results show that a frequency bandwidth of 2 THz and a large angle range of 10°, with an extinction ratios over 20 dB and a diffraction efficiencies over 90%, are obtained. This is a relatively well designed PBS in THz region.

2.2 Fabrication tolerance analysis

In the process of PBS manufacture, there would be unavoidable deviations of the geometric parameters, which may affect its properties, i.e. the diffraction efficiencies and extinction ratios. Therefore, detailed analyses on the parameters tolerances are extremely necessary.

In this way, contour maps in Fig.4 (a) –(d) respectively show the variations of T_0^{TM}, R_0^{TE}, T_c and R_c as a function of duty cycle f and frequency H, with the incident angle at 70° and other parameters kept the optimized ones. When f changes from 0.33 to 0.35, the values of T_0^{TM} are higher than 95.2% in the operating frequency range (from 3.5 THz to 5.5 THz), and meanwhile, the values of R_0^{TE} are more than 98.2%. What's more, the values of T_c are kept higher than 28 dB in this frequency range and the values of R_c are higher than 21 dB. Around the optimized value of f(f=0.34), the R_c reaches its maximum values 60 dB.

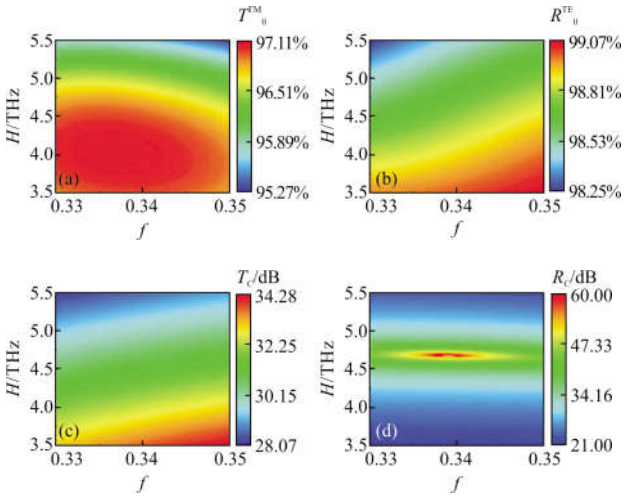

Fig.4 (a) T_0^{TM}, (b) R_0^{TE}, (c) T_c and (d) R_c versus the incident frequencies H and duty cycle f of the PBS whose D_1=2.9 μm, D_2=1.91 μm, D_3=1.12 μm, and Λ=6 μm, working at the incident angle θ=70°

We then calculate the diffraction efficiencies and extinction ratios when changing the groove depth D_2 from 1.8 μm to 2 μm, and fixing the other parameters. Figure 5 shows the corresponding results from 3.5 THz to 5.5 THz with the incident angle at 70°. As shown in Fig.5(a) and (b), the values of T_0^{TM} maintain higher than 95.4% and those of R_0^{TE} are more than 98.4%. Meanwhile, as shown in Fig.5(c) and (d), the values of T_c are higher than 27.8 dB and those of R_c are higher than 20.8 dB.

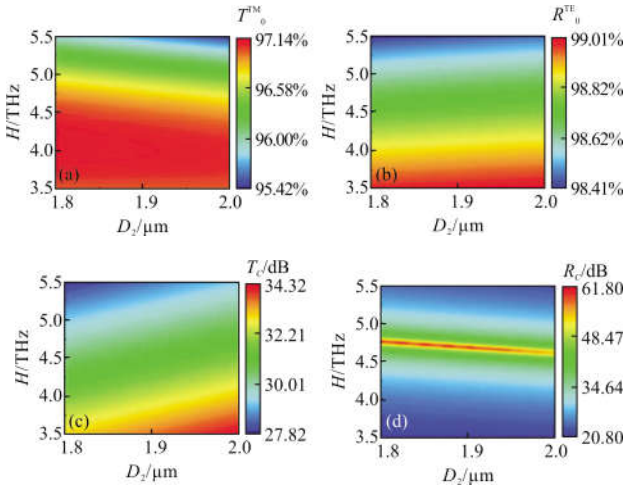

Fig.5 (a) T_0^{TM}, (b) R_0^{TE}, (c) T_c and (d) R_c versus the incident frequencies H and the groove depth D_2 of the PBS whose D_1=2.9 μm, D_3=1.12 μm, Λ=6 μm, and f=0.34 μm, working at incident angle θ=70°

After that, we analyze the dependence of T_0^{TM}, R_0^{TE}, T_c and R_c on the grating period Λ and the incident angle θ at 4.5 THz, while other parameters are kept constant. When the Λ varies from 5.9 μm to 6.1 μm and the θ ranges from 65° to 75°, the corresponding results are shown in Fig.6. Figure 6(a) and (b) reveal the values of T_0^{TM} are higher than 94.9% and those of

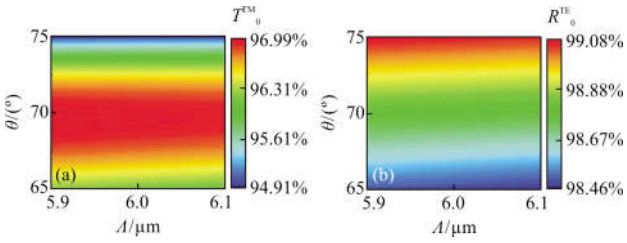

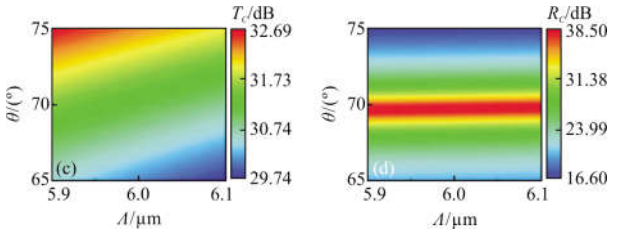

Fig.6 (a) T_0^{TM}, (b) R_0^{TE}, (c) T_c and (d) R_c versus the grating period Λ and incident angles θ of the PBS whose f=0.34, D_1=2.9 μm, D_2=1.91 μm, and D_3=1.12 μm, working at 4.5 THz

R_0^{TE} are higher than 98.4%. In the same range as displayed in Fig.6 (c) and (d), the values of T_c are higher than 29.7 dB and those of R_c are higher than 16.6 dB. Especially in the angle range from 65° to 73.5°, R_c are kept higher than 20 dB.

The contour maps in Fig.7 reveal the values of the diffraction efficiencies and extinction ratios as a function of the thickness D_1 (from 1 μm to 1.2 μm) and thickness D_3 (from 2.8 μm to 3 μm), at 4.5 THz with the incident angle of 70°. Figure 7 (a) and (b) show that the values of T_0^{TM} are always more than 96.9% and those of R_0^{TE} are more than 98.7%. Figure 7(c) and (d) exhibit that the values of T_c and R_c are respectively kept higher than 31 dB and 33.4 dB.

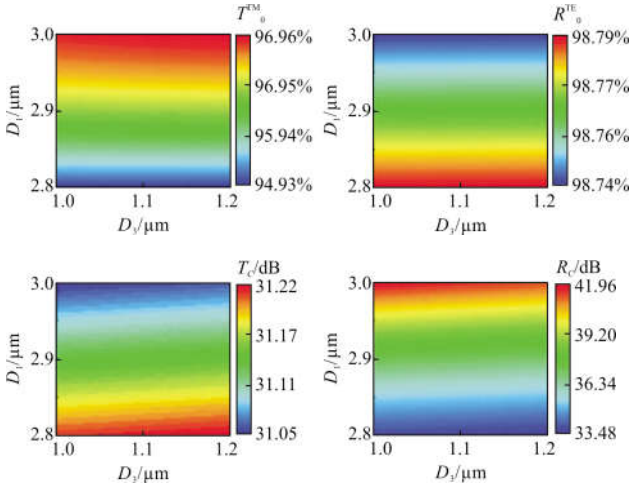

Fig.7 (a) T_0^{TM}, (b) R_0^{TE}, (c) T_c and (d) R_c versus the thickness D_1 and thickness D_3 of the PBS whose f=0.34, Λ=6 μm, and D_2=1.91 μm, operating at 4.5 THz with incident angle θ=70°

From the perspective above, our designed PBS has good manufacture tolerances of the duty cycle, groove depth, period and the thickness of the silica layers. In this way, this PBS device made of cheap materials owning low loss can be easily fabricated.

3 Conclusions

In this paper, a new PBS based on subwavelength grating sandwiched between dielectric layers is theoretically designed using RCWA, and optimized by GA. This PBS has relatively simple structure made by materials with low cost. The calculation results show that the designed PBS operating well in a broad band from 3.5 to 5.5 THz, with high diffraction efficiency and extinction ratios. Moreover, fabrication error analysis shows that the PBS has good tolerance in this respect. Therefore, this PBS may achieve wide applications in THz laser system, imaging system and polarization system.

References:

[1] Yardimci N T , Cakmakyapan S, Hemmati S, et al. A high-power broadband terahertz source enabled by three-dimensional light confinement in a plasmonic nanocavity[J]. ***Scientific Reports***, 2017, 7(1): 4166.

[2] Seifert T, Jaiswal S, Sajadi M, et al. Ultrabroadband single-cycle terahertz pulses with peak fields of 300 kV·cm $^{-1}$ from a metallic spintronic emitter [J]. ***Applied Physics Letters***, 2017, 110(25): 355-362.

[3] Lin Xufin, Zhou Fen, Zhang Jianbin, et al. High power wideband terahertz sources based on femtosecond facility[J]. ***Infrared and Laser Engineering***, 2012, 41(1): 116-118. (in Chinese)

[4] Zhang X, Tian Z, Yue W, et al. Broadband terahertz wave deflection based on C-shape complex metamaterials with phase discontinuities [J]. ***Advanced Materials***, 2013, 25(33): 4567-4572.

[5] Fan R H, Zhou Y, Ren X P, et al. Freely tunable broadband polarization rotator for terahertz waves [J]. ***Advanced Materials***, 2015, 27(7): 1201-1206.

[6] Neu J, Krolla B, Paul O, et al. Metamaterial-based gradient index lens with strong focusing in the THz frequency range [J]. ***Optics Express***, 2010, 19(5): 27748-27757.

[7] Scherger B, Jördens C, Koch M. Variable-focus terahertz lens[J]. ***Optics Express***, 2011, 19(5): 4528-4535.

[8] Fattinger C, Grischkowsky D, Exter M V, et al. Far-infrared time-domain spectroscopy with terahertz beams of dielectrics and semiconductors [J]. ***Journal of the Optical Society of America B***, 1990, 7(10): 2006-2015.

[9] Luo Zhiwei, Gu Xinan, Zhu Weichen, et al. Optical properties of GaSe: S crystals in terahertz frequency range [J]. ***Optics and Precision Engineering***, 2011, 19 (2): 354-359. (in Chinese)

[10] Rutz F, Hasek T, Koch M, et al. Terahertz birefringence of liquid crystal polymers[J]. ***Applied Physics Letters***, 2006, 89 (22): 221911.

[11] Mo G Q, Li J S. Compact terahertz wave polarization beam splitter using photonic crystal [J]. ***Applied Optics***, 2016, 55 (25): 7093-7097.

[12] Hou Yu, Yang Huijing. Broadband terahertz polarization splitter based on orthogonal dual hollow core [J]. ***Infrared and Laser Engineering***, 2016, 45(12): 1225005. (in Chinese)

[13] Wang W L, Rong X H. Design of terahertz wave polarizer based on thin film structure with micrometer [J]. ***Journal of Nanoengineering and Nanosystems***, 2014, 230(2): 81-84.

[14] Berry C W, Jarrahi M. Broadband terahertz polarizing beam splitter on a polymer substrate [J]. ***Journal of Infrared and Millimeter Terahertz Waves***, 2012, 33(2): 127-130.

[15] Du Mingdi, Jia Yaqiong, He Shuzhen. Impact of groove depth of subwavelength metal grating on THz spoof SPPs[J]. ***Infrared and Laser Engineering***, 2017, 46(8): 0825003. (in Chinese)

[16] Okamoto K, Tsuruda K, Diebold S, et al. Terahertz sensor using photonic crystal cavity and resonant tunneling diodes [J]. ***Journal of Infrared and Millimeter Terahertz Waves***, 2017, 38(9): 1085-1097.

[17] Pan Wu, Zeng Wei, Zhang Jun, et al. Design of multilayer stacked terahertz communication lens antenna [J]. ***Optics and Precision Engineering***, 2017, 25(1): 65-72. (in Chinese)

[18] Arnold M, Hehl K. Embedded grating in a multilayer system [J]. ***J Mod Opt***, 2007, 40(12): 2423-2432.

[19] Awasthi S K, Srivastava A, Malaviya U, et al. Wide-angle, broadband plate polarizer in terahertz frequency region [J]. ***Solid State Commun***, 2008, 146(11): 506-509.

[20] Knop K. Rigorous diffraction theory for transmission phase gratings with deep rectangular grooves [J]. ***J Opt Soc Am***, 1978, 68(9): 1206-1210.

[21] Hartke B. Global geometry optimization of clusters using genetic algorithms [J]. ***Iran J Public Health***, 1993, 97(39): 9973-9976.

[22] Zhou L b, Liu W. Broadband polarizing beam splitter with an embedded metal-wire nanograting [J]. ***Opt Express***, 2005, 30(12): 1434-1436.